

Cramér-Rao Lower Bound for UWB Delay Estimation in Multipath Conditions

Yochay Lustmann and Dana Porrat

School of Engineering and Computer Science, The Hebrew University, Jerusalem, Israel

Abstract—The accuracy of wide band propagation delay estimation is characterized. The Cramér-Rao Lower Bound (CRLB) for delay estimation in multipath conditions is presented in terms of the Ricean K-factor, the ratio of direct to diffuse multipath components. The validity of the derivation is demonstrated using thousands of measurements, where the K-factor is estimated in the spectral domain.

Index Terms—Electromagnetic propagation, Indoor radio communication, Multipath channels, Distance measurement.

I. INTRODUCTION

The most popular ultra wideband (UWB) channel measurement technique uses a vector network analyzer (VNA) that operates in the frequency domain, i.e. by frequency-sweeping the transmitted signal. The inherent averaging of the VNA reduces the sensitivity to noise and allows relatively high SNR [1]. This high SNR leaves the multipath phenomenon as the main cause of error for propagation delay estimation even in line of sight (LoS) conditions.

The Cramér-Rao Lower Bound (CRLB) provides a theoretical limit for the standard deviation of unbiased estimators, and can be used to derive a lower bound on the standard deviation of the error in estimating the propagation delay.

Theoretical derivations of the CRLB for UWB ranging are presented in [2]–[7]. The CRLB over an additive white Gaussian noise (AWGN) channel (no multipath) is developed in [2], and also presented in [3] and [4] that are based on earlier work. The CRLB for the estimation of the amplitudes and delays of the multipath components is developed by [5] and [6], both give complex formulas that are difficult to apply.

The main contribution of this paper is the derivation of a CRLB for UWB propagation delay in a Rice channel environment. The bound has a simple form that depends on the Ricean K-factor, a single parameter that is easy to characterize. A large number of measurements validate our results.

II. NOISE VS. MULTIPATH IN FREQUENCY DOMAIN CHANNEL MEASUREMENTS

When measuring the LoS radio channel in the frequency domain, i.e. by frequency sweeping/hopping methods, the

SNR is usually very high and noise influence on the ranging accuracy can be neglected. On the other hand, the influence of the multipath propagation may be significant. An example of channel phase measured in LoS conditions in an office is demonstrated in Figure 1 together with a simulation of the expected free space result. The phase correlation between neighboring frequencies is an indication that the main cause of error is not white noise. In order to be convinced that this deviation is not caused by phase drift of the VNA, the same measurement was conducted repeatedly five times. The pattern seen in Figure 1 was repeated very accurately.

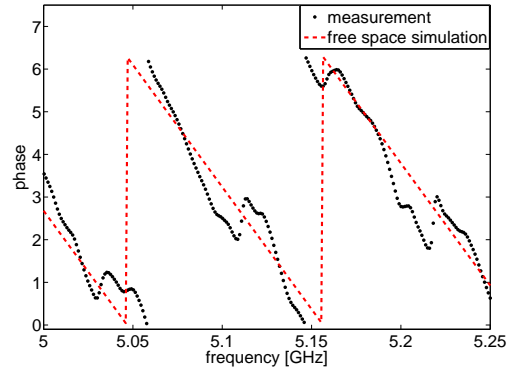


Fig. 1. Example of LoS measured phase versus frequency and an appropriate free space simulation.

A. The Rice Channel Model

The received signal can be described in the frequency domain using the transmitted signal $\tilde{S}(f)$ and the transfer function of the channel $\tilde{H}_{\tilde{\tau}}(f)$. Omitting the additive noise we have

$$\Psi_{\tilde{\tau}}(f) = \tilde{S}(f)\tilde{H}_{\tilde{\tau}}(f) \quad (1)$$

Where $\tilde{\tau}$ is the propagation delay between transmitter and receiver and f is the frequency.

The Ricean channel model is well-established for spatially distributed terminals in a line of sight multipath environment, and its applicability in the frequency domain was shown in [8]. The far-field channel response is modeled as complex normal:

$$\tilde{H}_{\tilde{\tau}}(f) \sim \mathcal{CN}\left(\frac{\alpha e^{-i2\pi f \tilde{\tau}}}{\tilde{\tau} c_0}, 2\tilde{\sigma}^2\right) \quad (2)$$

where α is a constant, c_0 is the speed of light and $R = \tilde{\tau}c_0$ is the transmitter-receiver separation. The $1/R$ dependence stems from energy preservation considerations. The variance $2\tilde{\sigma}^2$ represents the multipath (diffuse) components of the channel. The Ricean channel model is justified using a large number of independent and identically-distributed multipath components, that combine into a Gaussian. We assume that $\tilde{\sigma}$ does not depend on frequency, in fact a weak frequency dependence is shown in [8].

In order to circumvent the singularity at $R = 0$ we use a calibrated version of the channel response, that is normalized by the response at a transmitter-receiver separation R_c .

The far-field calibrated channel response is

$$H_\tau(f) = \frac{\tilde{H}_{\tilde{\tau}}(f)}{\tilde{H}_{R_c/c_0}(f)} \quad (3)$$

and the calibrated propagation delay:

$$\tau = \tilde{\tau} - \frac{R_c}{c_0} \quad (4)$$

The calibrated received signal in the frequency domain:

$$\Psi_\tau(f) = \left[\tilde{S}(f) \tilde{H}_{R_c/c_0}(f) \right] H_\tau(f) = S(f) H_\tau(f) \quad (5)$$

where $S(f)$ represents the signal at distance R_c from the transmitter.

The calibrated channel is now modeled by:

$$H_\tau(f) \sim \mathcal{CN}(Ae^{-i2\pi f\tau}, 2\sigma^2) \quad (6)$$

where

$$A = \frac{R_c}{\tau c_0 + R_c} \quad (7)$$

The variance $2\sigma^2$ does not depend on frequency as the calibration (3) has a frequency-independent amplitude.

III. CRAMÉR-RAO LOWER BOUND

The CRLB provides a theoretical limit for the standard deviation of unbiased estimators. When using N frequencies, the received signal can be presented using a real vector:

$$\vec{\Psi}_\tau = \begin{pmatrix} \text{Re}[\Psi(f_1)] \\ \text{Im}[\Psi(f_1)] \\ \vdots \\ \text{Re}[\Psi(f_N)] \\ \text{Im}[\Psi(f_N)] \end{pmatrix} \quad (8)$$

$$\begin{aligned} \vec{\mu}_\tau &= \text{mean}(\vec{\Psi}_\tau) \\ &= \begin{pmatrix} \text{Re}[S(f_1)Ae^{-i2\pi f_1\tau}] \\ \text{Im}[S(f_1)Ae^{-i2\pi f_1\tau}] \\ \vdots \\ \text{Re}[S(f_N)Ae^{-i2\pi f_N\tau}] \\ \text{Im}[S(f_N)Ae^{-i2\pi f_N\tau}] \end{pmatrix} \end{aligned} \quad (9)$$

The covariance matrix is diagonal for frequencies that are far enough apart, i.e. separated further than the coherence bandwidth:

$$C_\Psi = \sigma^2 \begin{pmatrix} |S(f_1)|^2 & & & 0 \\ & |S(f_1)|^2 & & \\ & & \dots & \\ 0 & & & |S(f_N)|^2 \\ & & & & |S(f_N)|^2 \end{pmatrix} \quad (10)$$

The Fisher information for a multivariate normal distribution with a constant covariance matrix has the form:

$$\begin{aligned} \mathcal{I}(\tau) &= \left[\frac{\partial \vec{\mu}_\tau}{\partial \tau} \right]^\top C_\Psi^{-1} \left[\frac{\partial \vec{\mu}_\tau}{\partial \tau} \right] \\ &= 2K \sum_{j=1}^N \left[4\pi^2 f_j^2 + \left(\frac{c_0 A}{R_c} \right)^2 \right] \end{aligned} \quad (11)$$

$$K = \frac{A^2}{2\sigma^2} \quad (12)$$

Where K is the Ricean K-factor of the channel.

The Fisher information can be described as the sum of phase and amplitude components:

$$\mathcal{I}(\tau) = \mathcal{I}_\phi(\tau) + \mathcal{I}_A(\tau) \quad (13)$$

$$\mathcal{I}_\phi(\tau) = 8\pi^2 K \sum_{j=1}^N f_j^2 \quad (14)$$

$$\mathcal{I}_A(\tau) = 2NK \left(\frac{c_0 A}{R_c} \right)^2 \quad (15)$$

For our measurements $R_c = 0.45$ m, the minimum frequency is 3 GHz and of course $A \leq 1$. Under these conditions we have per frequency:

$$\mathcal{I}_\phi(\tau) \geq 7.1 \cdot 10^{20} K \frac{1}{\text{sec}^2} \quad (16)$$

$$\mathcal{I}_A(\tau) \leq 8.9 \cdot 10^{17} K \frac{1}{\text{sec}^2} \quad (17)$$

It is clear that the amplitude component (15) of the Fisher information can be neglected. The lower bound for the standard deviation of the propagation delay is the reciprocal of the square-root of the Fisher information:

$$\Sigma_\tau \geq \frac{1}{\sqrt{\mathcal{I}_\phi(\tau)}} = \frac{1}{2\sqrt{2}\pi \sqrt{\sum_{j=1}^N f_j^2}} \frac{1}{\sqrt{K}} \quad (18)$$

Section V-D validates (18) using channel measurements.

IV. MEASUREMENT ENVIRONMENT AND EQUIPMENT

A. The System and the Measurement Environment

The measurement setup was based on an Agilent N5230 vector network analyzer (VNA), connected to two omnidirectional antennas (Electro-Metrics EM-6865) and suitable amplifiers. The VNA transmitted sinusoidal waves in the 3-7 GHz band with a frequency step of 1062.5 KHz (total of 3767 frequencies). Each frequency was transmitted for about 0.02

seconds (the reciprocal of the VNA intermediate frequency bandwidth), and the relative amplitude and phase, compared to the transmitted signal, were recorded. The SNR was higher than 34 dB in all measurements and the coherence bandwidth was between 25 to 85 MHz.

The receive antenna (Rx) was placed on a linear motorized positioner with sub-millimeter accuracy, that was one meter long. The receiver was moved between measurements but kept immobile during the collection of each channel response. The transmit antenna (Tx) was placed on a cart that was moved to different locations for different measurements, but was immobile during each measurement. The Tx and Rx antennas were placed 1.25 m above the floor. We put the transmitter in the same room with a receiver array, in an 'end-fire' position, i.e. along the line connecting all receiver positions.

A computer controlled the location of the receive antenna along the rail, as well as the parameters of the VNA and the storage of channel data.

The measurements used in this paper were collected in 2008-2009 in the Ross building at Givat Ram campus of the Hebrew University of Jerusalem. We made about 14,700 LoS measurements in two office rooms, with 57 different cart (Tx) and motorized rail (Rx) positions. Measurements were normally performed during nights, with no movement of people around the system.

B. Calibration

We used a Line of Sight (LoS) measurement with about 45 cm between receiver and transmitter antennas to calibrate the system. The radiation pattern of a biconical antenna is similar to that of a short dipole [9], and its far field boundary is thus about $\frac{\lambda}{2}$, below the calibration distance of 45 cm over the entire measurement band. This calibration method allows to calibrate out the cable and antenna responses but has the disadvantage of including multipath components. In order to alleviate this difficulty we transformed the calibration measurement to the time domain using a rectangular window, cut out the multipath components (by eliminating the small amplitudes that come after the main pulse), and transformed it back to the frequency domain. We got a calibration response that was used as follows:

$$r_f = \frac{r_f^{(measurement)}}{r_f^{(calibration)}} \quad (19)$$

$$\phi_f = \phi_f^{(measurement)} - \phi_f^{(calibration)} \quad (20)$$

Where r_f is the amplitude and ϕ_f is the phase for the frequency f .

The distance between Tx and Rx during calibration is denoted R_c , and after the calibration process we consider each transmitted sinusoidal wave as if it had amplitude 1 and phase 0 at distance R_c from the transmitter.

V. RESULTS

A. Propagation Delay Correlation

For propagation delay measurements where the main cause of error is white noise, estimates from neighboring Rx po-

sitions are uncorrelated. For channel measurements where the main cause of deviation from free space is multipath propagation, the phase is correlated across small distances and frequency steps on the order of the coherence bandwidth. This correlation may distort the estimation of the standard deviation of the propagation delay error. In order to reduce the correlation of our propagation delay estimates, we randomly selected the frequencies used per each measurement, using a unique set of frequencies per Rx position. From the 3767 measured frequencies we randomly selected 188, and used them to evaluate $\hat{\tau}$ as explained below in Section V-B.

B. Propagation Delay Error

In order to estimate the propagation delay we measured the channel responses between a stationary transmitter and a receiver array as described in Section IV-A. For each receiver position (x_k) we measured the amplitude (r_f) and phase (ϕ_f) of the channel response in the band of 3 - 7 GHz with steps of 1062.5 KHz (total of 3767 frequencies), and randomly selected 188 frequencies as described above. A measurement example is demonstrated in Figure 2.

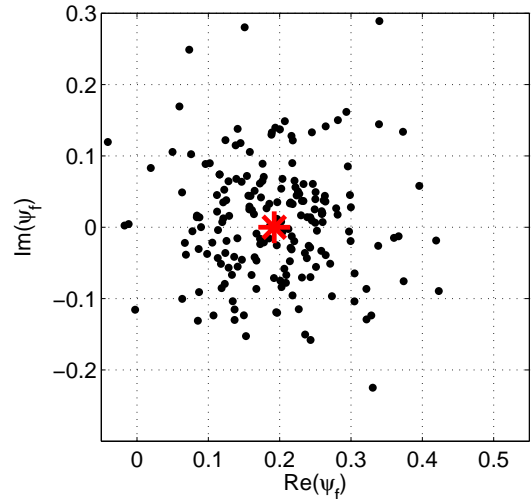


Fig. 2. Example of a 188 complex channel responses taken from a single LoS measurement. Each black dot represents $r_f e^{i(\phi_f - 2\pi f \hat{\tau})}$ measured at a different frequency, and the star is the center of mass of all the dots.

The propagation delay (τ) was estimated using a cosine transform, that is similar to an inverse Fourier transform, by looking for the peak position in the time domain¹:

$$\hat{\tau} = \arg \max_t \left(\sum_f r_f \cos [2\pi f t - \phi_f] \right) \quad (21)$$

We estimated the distance of the k-th receiver from the calibration point² $\hat{R}(x_k)$

$$\hat{R}(x_k) = c_0 \hat{\tau}(x_k) \quad (22)$$

¹In line of sight the first multipath component is also the strongest.

²We calibrated the system so that $\tau=0$ at distance R_c from the transmitter.

Now using the Matlab 'fit' function we fitted $\hat{R}(x_k)$ to a linear function³ $\rho(x_k)$, and estimated the error of the propagation delay:

$$\Delta\hat{\tau}_k = \frac{\hat{R}(x_k) - \rho(x_k)}{c_0} \quad (23)$$

C. K-Factor

The Ricean K-factor was extracted for each measurement as follows:

$$\hat{K}_k = \frac{\hat{A}_k^2}{2\hat{\sigma}_k^2} \quad (24)$$

Where

$$\hat{A}_k^2 = \left| \text{Mean}(r_f e^{i(\phi_f - 2\pi f \hat{\tau})}) \right|^2 \quad (25)$$

$$2\hat{\sigma}_k^2 = \text{Var}(r_f e^{i(\phi_f - 2\pi f \hat{\tau})}) \quad (26)$$

D. Propagation Delay Vs. K-Factor

Figure 3 presents the estimates of $\Delta\hat{\tau}_k$ versus \hat{K}_k . In order to compare our results with the theoretical CRLB

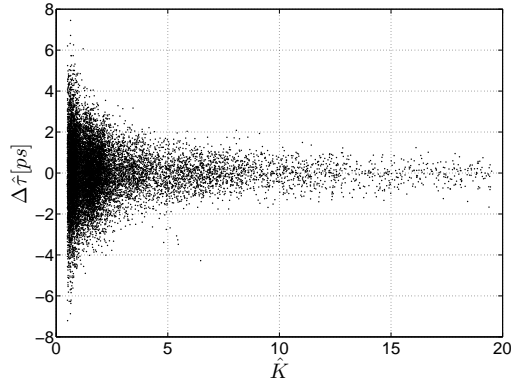


Fig. 3. Error in time of arrival versus the estimated Ricean K-factor. A timing error of 3.33 ps is equivalent to a ranging error of 1 mm.

we calculated the standard deviation of the propagation delay estimation error over small ranges of \hat{K} :

$$\Sigma_{\hat{\tau}} = \sqrt{\text{Var}(\Delta\hat{\tau})} \quad (27)$$

The results, together with the CRLB (18), are presented in Figure 4. We used a random set of frequencies for each measurement as explained in Section V-B, calculated $\sum_{j=1}^N f_j^2$ for each measurement, and used the maximum from our 14,700 Rx positions for the calculation of the bound.

³The slope of the linear function was very close to one because of the approximate alignment of the transmitter and the array of receivers.

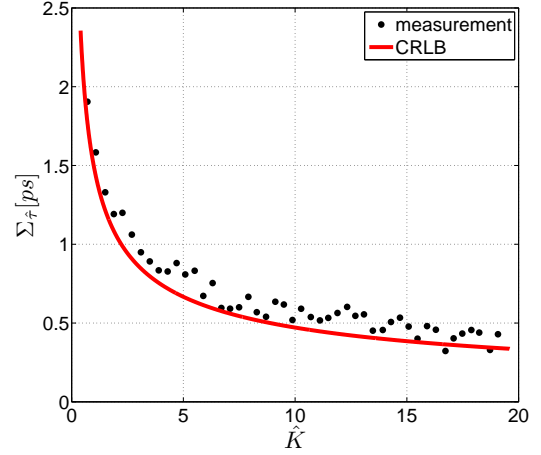


Fig. 4. Standard deviation of the error in propagation delay versus the Ricean K-factor. The standard deviation was calculated on steps of 0.4 K-factors from the results presented in Figure 3. The solid line is the CRLB from (18).

VI. CONCLUSION

This paper introduced the Cramér-Rao lower bound for UWB propagation delay estimation in LoS multipath channels, where the multipath intensity is represented by the Ricean K-factor. The validity of the CRLB was demonstrated using thousands of measurements performed in two office rooms. This bound should be considered when performing UWB time of arrival (ToA) localization with high SNR. The analysis produced sub-millimetric ranging accuracy, that is superior to other results in the literature.

REFERENCES

- [1] A. Molisch, "Ultrawideband propagation channels-theory, measurement, and modeling," *Vehicular Technology, IEEE Transactions on*, vol. 54, no. 5, pp. 1528–1545, Sept. 2005.
- [2] R. Cardinali, L. De Nardis, M.-G. Di Benedetto, and P. Lombardo, "UWB ranging accuracy in high- and low-data-rate applications," *Microwave Theory and Techniques, IEEE Transactions on*, vol. 54, no. 4, pp. 1865–1875, June 2006.
- [3] S. Gezici, Z. Tian, G. Giannakis, H. Kobayashi, A. Molisch, H. Poor, and Z. Sahinoglu, "Localization via ultra-wideband radios: a look at positioning aspects for future sensor networks," *Signal Processing Magazine, IEEE*, vol. 22, no. 4, pp. 70–84, July 2005.
- [4] Z. Şahinoğlu, S. Gezici, and I. Güvenç, *Ultra-Wideband Positioning Systems*. Cambridge University Press, 2008.
- [5] H. Celebi and H. Arslan, "Ranging Accuracy in Dynamic Spectrum Access Networks," *Communications Letters, IEEE*, vol. 11, no. 5, pp. 405–407, May 2007.
- [6] T. Kaiser and B. Sieskul, "Cramer-Rao bound for TOA estimations in UWB positioning systems," in *Ultra-Wideband, 2005. ICU 2005. 2005 IEEE International Conference on*, Sept. 2005, pp. 408–413.
- [7] J. Zhang, R. Kennedy, and T. Abhayapala, "Cramer-Rao lower bounds for the time delay estimation of UWB signals," in *Communications, 2004 IEEE International Conference on*, vol. 6, June 2004, pp. 3424–3428 Vol.6.
- [8] Y. Lustmann and D. Porrat, "Indoor channel spectral statistics, k-factor and reverberation distance," *IEEE Transactions on Antennas and Propagation*, to be published.
- [9] D. Ghosh and T. K. Sarkar, "Design of a wide-angle biconical antenna for wideband communications," *Progress In Electromagnetics Research B*, vol. 16, pp. 229–245, 2009.